

Microseconds–Nanoseconds All-Optical Switching of Visible-Near Infrared (0.5 μm –1.55 μm) Lasers with Dye-Doped Nematic Liquid Crystals

I. C. KHOO, J. LIOU, AND M. V. STINGER

Electrical Engineering Department, The Pennsylvania State University,
University Park, Pennsylvania, USA

Laser induced disorder is an efficient and very fast mechanism to induce changes in the birefringence of nematic liquid crystals, which in turn enable many nonlinear optical processes. Using a 90-degrees twist alignment nematic liquid crystal doped with suitable dye to impart the required photonic absorption and order parameter modulation, we have demonstrated ultrafast all-optical shuttle operation for lasers spanning the visible to near-infrared spectral region (532 nm; 488 nm; 750 nm; 1060 nm; 1550 nm). With increasing intensity, the on-time of the switch decreases from microseconds to the nanoseconds regime, in such a manner that the transmitted light energy/intensity is clamped to below the eye- or sensor-safe levels.

Keywords All-optical switching; birefringence; microseconds; nanoseconds; order-disorder; visible – infrared lasers

I. Introduction

Liquid crystals possess extraordinarily large optical nonlinearities that span over multiple time scales – from femtoseconds, picoseconds, through nanoseconds, microseconds to the cw regime [1–10]. In ordered phases such as nematics, laser induced director axis reorientation and order parameter changes give rise to nonlinear refractive index coefficients that are many orders of magnitude larger than all known nonlinear optical materials [1,2]. Such extraordinarily large electronic and non-electronic nonlinearities have enabled many nonlinear processes not possible with other existing materials. To date, almost all conceivable nonlinear optical phenomena have been observed in a very broad spectrum spanning the entire visible to infrared, including self-phase modulations, focusing, defocusing, soliton propagation, photorefractivities and supra-nonlinearities, beam combining, slow and fast light, nonlinear dynamics, bistabilities and instabilities, chaos, and a host of coherent wave mixing and image processing effects [13–24].

Among the self-action effects observed to date, all-optical switching processes in which an incident laser self attenuates as it propagates through the liquid material/device by inducing changes in the material's optical properties [e.g., intensity

Address correspondence to I. C. Khoo, Electrical Engineering Department, The Pennsylvania State University, University Park, PA 16802. E-mail: ick1@psu.edu

dependent refractive index or birefringence] are potentially useful for practical application in sensor protection against intense lasers [4,5,15,25–27]. We have previously [25–27] demonstrated that twist alignment nematic liquid crystal (TNLC) in combination with crossed polarizers would perform such functions, for lasers in the visible [e.g., 488 nm, 532 nm] as well as infrared [1550 nm]. The underlying mechanism—laser induced temperature and order parameter modification, leading to diminished birefringence—is a much faster process than director axis reorientation, and enable microseconds switching times with increasing input laser intensity. Since the birefringence of NLC spans the entire visible–infrared spectrum [2], such self-action optical switching processes can be realized throughout this spectral regime. In this paper, we report newly obtained results/demonstrations with near infrared lasers ($\lambda = 1060$ nm and $\lambda = 750$ nm), further demonstrating the broadband applicability of such birefringence mediated switching process. More importantly, we also demonstrate for the first time that the transmission switching in these bulk nematic liquid crystal cells can be as fast as 20 ns with moderate power laser.

II. All-Optical Switching by Laser Induced Disorder

Figure 1 depicts the experimental set up for the all-optical switching process involving a 90° twist alignment nematic liquid crystal placed between two crossed polarizer similar to that reported in reference [26]. A linearly polarized laser is incident at normal to the sample with its polarization axis parallel to the nematic director axis (along x-axis). The liquid crystals used is 5CB (Pentyl-Cyano-Biphenyl) and is doped with various dyes that absorb at the laser wavelength used (e.g., Methyl-red for visible [27]; IR-99 for $1.55\mu\text{m}$ [26]; Epolite dye for $\lambda = 1060$ nm; ‘IR-780 Iodide’ dye for 750 nm in this paper). At low optical power, the polarization vector obeys the

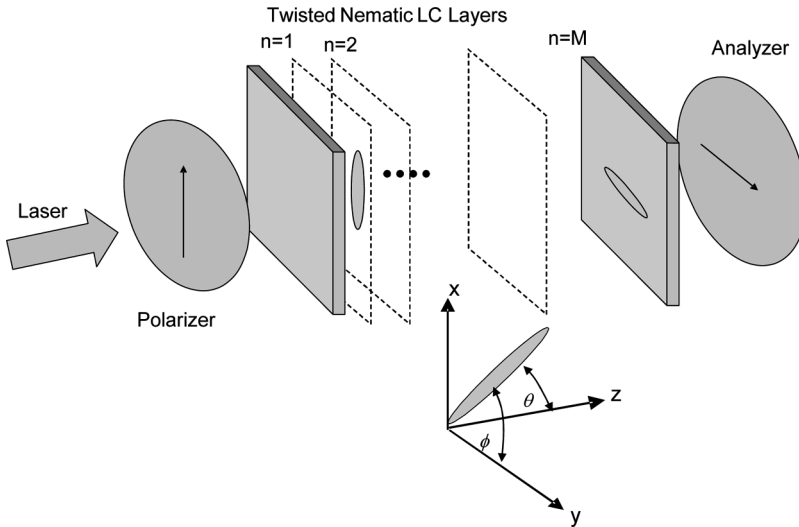


Figure 1. Schematic depiction of the nonlinear propagation of a linearly polarized light through a 90° twist alignment nematic liquid crystal cell.

Mauguin rule and rotates in accordance to the nematic axis, and emerges with a 90° rotation which is maximally transmitted by the exit analyzer (transmission axis along y-axis). If the input laser intensity is high enough to cause significant birefringence change and director axis and order parameter fluctuations, the polarization rotation process will be degraded and the transmission through the exit polarizer will decrease, eventually diminishes to vanishing value when the order parameter (and therefore the birefringence) $\rightarrow 0$.

To quantitatively describe this process, we have developed a modified Jones Matrix method as detailed in previous publications [26]. Following the Jones Matrix method, the liquid crystal cell is divided into M layers with thickness h . The amplitude of the normalized transmitted light through the entire (polarizer + LC film + analyzer) set up is given by:

$$\Psi_{out}(d) = \begin{pmatrix} E'_x \\ E'_y \end{pmatrix} = P(\phi_{Exit}) \cdot \prod_{m=1}^M [S^{-1}(\phi_m) \cdot G \cdot S(\phi_m)] \cdot \begin{pmatrix} \cos \phi_{Ent} \\ \sin \phi_{Ent} \end{pmatrix} \quad (1)$$

where

$$P(\phi) = \begin{pmatrix} \cos^2 \phi & \cos \phi \sin \phi \\ \sin \phi \cos \phi & \sin^2 \phi \end{pmatrix}; \quad S(\phi_m) = \begin{pmatrix} \cos \phi_m & \sin \phi_m \\ -\sin \phi_m & \cos \phi_m \end{pmatrix};$$

$$G = \begin{pmatrix} e^{i\frac{\gamma}{2}} & 0 \\ 0 & e^{-i\frac{\gamma}{2}} \end{pmatrix}. \quad (2)$$

In these equations, $\gamma = 2\pi h \Delta n_m / \lambda$ is the retardation associated with the m -th LC layer

$$\Delta n_m = \frac{n_e n_o}{\sqrt{n_e^2 \sin^2 \theta_m + n_o^2 \cos^2 \theta_m}} - n_o \quad (3)$$

and θ_m and ϕ_m are the tilt and twist angle of m -th layer director axis and ϕ_{Ent}, ϕ_{Exit} are the axis of the entrance polarizer and exit analyzer, respectively ($\phi_{Ent} = 90^\circ$ and $\phi_{Exit} = 0^\circ$).

The birefringence of the m -th layer at time t is governed by the local temperature T and order parameter S , i.e., $\Delta n_m(t) = \Delta n(S, T)$. The order parameter of the NLC could also be affected by the presence of the Cis-species if the nematic liquid crystal is doped with azo-molecules that could under trans-cis isomerism upon photo-excitation, i.e., $S = S(I(t), T(t); N_{T,C}(t))$ where $N_{T,C}$ = Number densities of Trans- and Cis species.

In a previous publication [26], we have considered the case where the order parameter is a function of the temperature T only, through the following coupled Eqs. (4) and (5)

$$\rho_0 C_p \frac{\partial T(\vec{r}, t)}{\partial t} - k \nabla^2 T(\vec{r}, t) = \dot{q} = \alpha I(\vec{r}) \quad (4)$$

$$f(S(z)) = a(T(z) - T^*)S(z)^2 + BS(z)^3 + CS(z)^4 \\ + L\left(\frac{dS(z)}{dz}\right)^2 - G_1S_1 - G_2S_2 \quad (5)$$

with boundary conditions:

$$-\left(\frac{\partial f}{\partial(\partial S/\partial z)}\right)_1 + \frac{\partial f_{S_1}}{\partial S_1} = 0, \quad \text{and} \quad \left(\frac{\partial f}{\partial(\partial S/\partial z)}\right)_2 + \frac{\partial f_{S_2}}{\partial S_2} = 0 \quad (6)$$

The time dependent order parameter changes associated with the time and 3-D spatial dependence of the temperature build up following laser absorption is a complex issue, and numerical modeling is needed in all cases. These theoretical modeling using experimental results are currently underway; details will be presented in a longer article elsewhere. It suffices to say that if the laser induced switching process occurs in a time scale shorter than the characteristics diffusion time constant, one could simplify the consideration by ignoring the spatial thermal diffusion, i.e., the changes in temperature and order parameter are local, and are dependent only on the time-integrated laser energy absorbed by the liquid crystal. Similar argument applies to the case where the disorder is created by laser excited Trans-Cis isomerism, where laser absorption gives rise to an increase in the Cis-species locally, if the build-up of the Cis-species takes place in a time shorter than the Trans-Cis species diffusion in the host medium. The local build-up of the Cis species gives rise to a local disorder (local changes in the order parameter).

III. All-Optical Switching of 750-nm and 1060-nm Lasers

Both theory and experiments have shown that the switch-off time depends on how fast the laser energy is deposited, c.f. Figure 2; the faster the energy is absorbed, the faster is the switch off [25,26]. The transmittance of the laser is nonlinearly [decreasing function] dependent on its incident intensity or energy. Previous experiments with visible lasers (4880 nm [ref. 27]; 532 nm ref. [26].) and communication wavelength laser (1550 nm [ref. 25]) have demonstrated that the extinction ratio can be > 1000 , while the switch off time can be as short as a few microseconds. We have recently conducted these switching processes in two spectral regions abound with intense laser sources, namely 1060 nm and 750 nm. Besides ‘filling in’ spectral gaps between 4880 nm and 1550 nm, we have demonstrated for the first time that these all-optical switching processes in thick (10’s microns) nematic liquid crystals can occur in a time scale as short as 20 nanoseconds with pulsed lasers.

III.A. All-Optical Switching with 750 Nm Step-On-CW and Pulsed Lasers

The liquid crystal used is 5CB in a planar 90° twist alignment, and is doped with traces of (~ 0.1 – 0.3% by weight) ‘IR-780 Iodide’ dye. With a cell thickness of $50\ \mu\text{m}$, the transmission at low input laser power ranges from 30–70% at 750 nm. Very thick samples, ranging from $100\ \mu\text{m}$ to $150\ \mu\text{m}$ with lower dye-dopant concentration have also been tested, yielding similar switching results. We summarize below some of the pertinent switching characteristics.

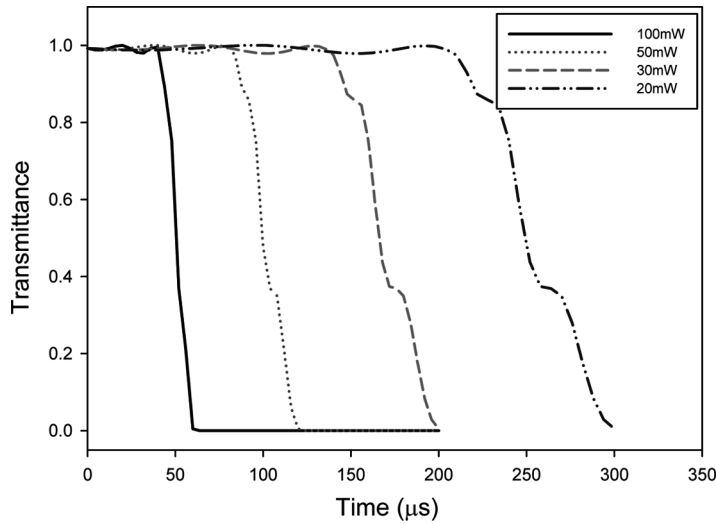


Figure 2. Theoretical plots of the normalized transmission as a function of time for increasing laser powers. Parameters used: laser power = 100 mW; focused beam radius 40 μm; $\alpha = 2 \times 10^4 \text{ m}^{-1}$; sample thickness $z = 50 \text{ μm}$, Initial temperature = 300 K.

Figure 3 shows the input (lower trace) and the transmitted output (upper trace) at the input power of 205 mW. An electronic shutter is used to turn on the cw 750 nm laser; as shown in the lower trace, the incident laser is ramped up to its maximum intensity level in $\sim 1 \text{ ms}$. The upper trace for the transmitted output laser power shows that it peaks at $\sim 400 \text{ microseconds}$ and subsequently ‘decays’ to $< e^{-2}$ of its

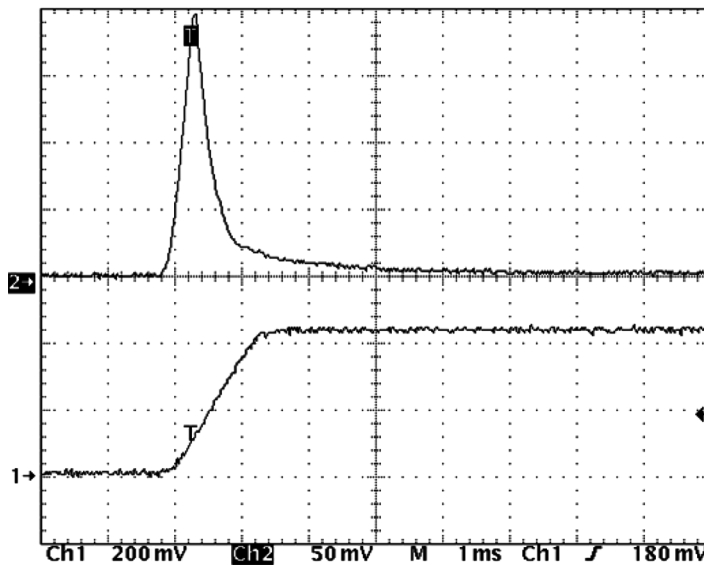


Figure 3. Oscilloscope traces of the transmitted [upper] and input [lower] cw lasers. Sample thickness: 50 μm; Dye concentration $\sim 0.3\%$; input power: 205 mW; laser wavelength: 750 nm.

peak value in ~ 400 microseconds. The peak transmitted power is measured to be 21 mW. The total transmitted laser energy is therefore $\sim 400 \times 10^{-6} \times 21 \times 10^{-3}$ joule $\sim 0.8 \mu\text{J}$, which is below the MPE (Maximum Permissible Exposure) of the eye [28]. Similar results/trends are obtained as we vary the input laser power; the higher is the power, the faster is the switching off dynamics, with 'clamped' transmitted laser energy below the μJ level.

To investigate such switching trend further, we employ a q-switched 750 nm laser with pulse duration of ~ 250 nanoseconds. The laser focal spot diameter on the TNLC sample is $140 \mu\text{m}$. Figure 4a-b show the input (upper trace) and output (lower) pulses at low (0.2 mJ) and high (~ 3.5 mJ) input laser energy, respectively. At low input energy, there is no appreciable switching, and the output pulse follows the input pulse dynamics and assumes the same pulse shape and duration. On the other hand, at high input laser energy, the transmitted output laser pulse begins to

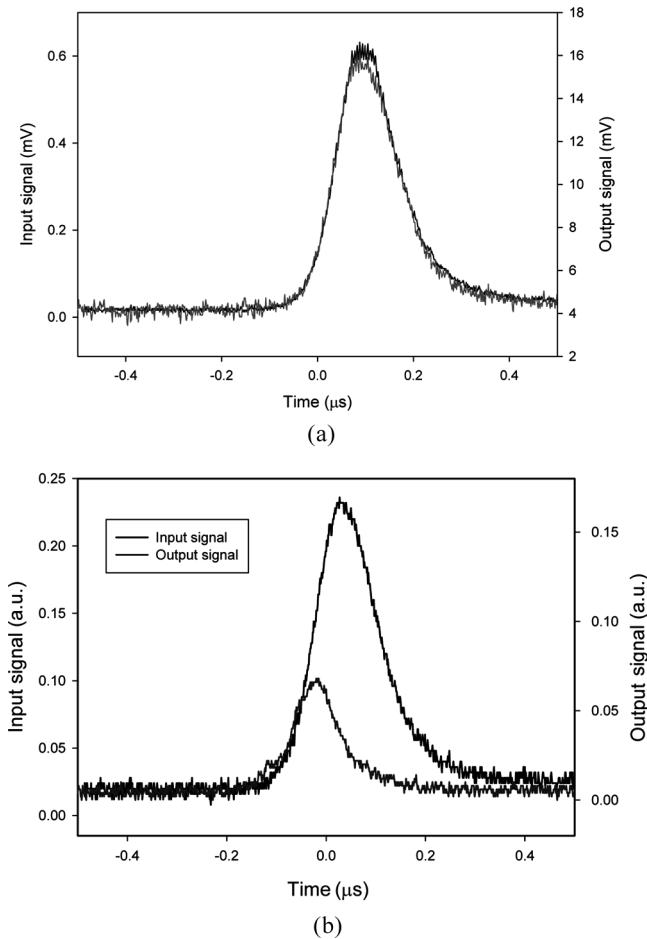


Figure 4. Oscilloscope traces of the transmitted and input laser pulses; laser wavelength: 750 nm, input pulse duration: 250 ns; LC cell thickness: $50 \mu\text{m}$; laser focused diameter: $140 \mu\text{m}$. (a) Input power: 0.2 mJ showing similar pulse shape. (b) Input power: 3.5 mJ showing clamped/switched off of the transmitted laser (lower trace).

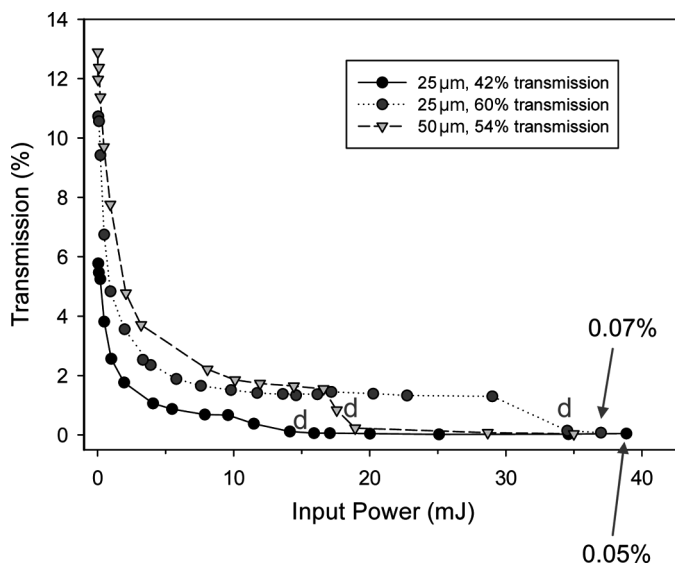


Figure 5. Measured transmissions of the 750 nm lasers as a function of the input laser energies for various cell thicknesses and initial transmission values [dye concentration].

exhibit significant reduced transmission in ~ 80 ns, with the later portion of the pulse completely diminished in ~ 50 ns. The transmission [output energy/input energy] as a function of the input energy for various sample thickness and initial (linear) transmission values are shown in Figure 5. These results all depict a highly desirable dependence for sensor protection application: the higher is the input, the lower is the transmission. At an input energy of ~ 30 mJ [energy fluence of 30 mJ/140 μm], the transmission switch-off occurs even faster (~ 25 ns). For this and higher input laser energies, the transmission drops below 0.1%, i.e., the extinction ratio is > 1000 . At these high input energies, however, the ‘superheated’ liquid in the focal region is often forced out of the region and/or damaged, but the crossed polarizer set up would still ensure extinction of the incident laser in the absence of the liquid crystal. Such pin-prick damage spot does not degrade the overall image transmission capability of the entire TNLC cell, nonetheless.

III.B. All-Optical Switching with Step-On CW 1060 Nm Laser

We close this paper with some preliminary demonstration of such all-optical switching effect with 1060 nm laser. In this case, a linearly polarized laser at this wavelength is incident on a 50 μm thick Epolite-dye doped liquid crystal (5CB) sample. The dye concentration used ranges from 0.25% to 0.1% by weight, and the low power transmission of the sample ranges from 35% to $\sim 60\%$. The focal spot diameter on the sample is 60 μm . As expected, similar transmission switching characteristics are obtained. Figure 6 shows the transmission as a function of the input laser power for the 0.25% doped sample. The switching threshold was measured to be ~ 300 μW , above which the transmission drops dramatically as the incident laser power is raised. The switching dynamics, extinction ratio, and other characteristics are similar to those reported previously for visible (532 nm) and infrared (1550 nm) lasers.

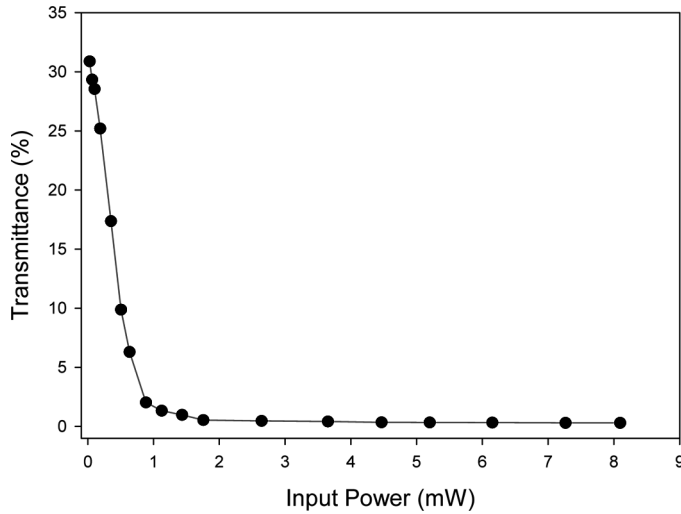


Figure 6. Measured transmission of the cw-1060 nm lasers as a function of the input laser power, showing high extinction switching. Laser spot diameter: 60 μm ; cell thickness: 50 μm .

IV. Conclusion Remarks

In conclusion, we have demonstrated all-optical switching capabilities of various dye-doped nematic liquid crystals in the visible – infrared spectral regime. The underlying mechanism is laser induced modulation of the birefringence, through order parameter changes associated with laser heating and/or dopant conformational changes. The switching threshold, extinction ratio and other dependencies on the input laser's temporal and power/energy are shown to be highly desirable for self-action sensor protection application. In particular, the transmission decreases and the switch-off times shorten with increasing input power/energy. Detailed theoretical modeling of the fundamental laser induced order parameter modulation dynamics for various sample geometry and laser characteristics are currently underway to arrive at optimal performance.

Acknowledgments

This work is supported by the Air Force Office of Scientific Research, the Army Research Office and the National Science Foundation Material Research Science and Engineering Center DMR-0820404.

References

- [1] Khoo, I. C. (2009). Nonlinear optics of liquid crystalline materials. *Physics Report*, 471, 221–267.
- [2] Khoo, I. C. (2007). *Liquid Crystals*, 2nd Ed., Wiley Inter-Science: NJ.
- [3] Khoo, I. C., Lindquist, R. G., Michael, R. R., Mansfield, R. J., & Lopresti, P. (1991). Dynamics of picosecond laser induced density, temperature and flow-reorientation effects in the mesophases of liquid crystals. *J. Appl. Phys.*, 69, 3853.

- [4] Khoo, I. C. (2008). Nonlinear organic liquid cored fiber array for all-optical switching and sensor protection against short pulsed lasers. *IEEE J. Selected Topics in Quantum Electronics JSTQE*, 14(3), 946–951.
- [5] Khoo, I. C., Webster, S., Kubo, S., Youngblood, W. J., Liou, J., Diaz, A., Mallouk, T. E., Lin, P., Peceli, D., Padilha, L. A., Hagan, D. J., & Van Stryland, E. W. (2009). Synthesis and characterization of the multi-photon absorption and excited-state properties of 4-propyl 4'-butyl diphenyl acetylene. *J. Mater. Chem.*, 19, 7525–7531.
- [6] Nersisyan, S. R., Tabiryan, N. V., Steeves, D. M., & Kimball, B. R. (2009). Optical axis gratings in liquid crystals and their use for polarization insensitive optical switching. *JNOPM*, 18, 1–47.
- [7] DeLuca, A., Barna, V., Ferjani, S., Caputo, R., Versace, C., Scaramuzza, N., Bartolino, R., Umeton, C., & Strange, G. (2009). Laser action in dye doped liquid crystals: From periodic structures to random media. *JNOPM*, 18, 349–365.
- [8] Khoo, I. C., Li, H., & Liang, Y. (1994). Observation of orientational photorefractive effects in nematic liquid crystals. *Optics Letts*, 19, 1723.
- [9] Lucchetti, L., Gentili, M., Simoni, F., Pavliuchenko, S., Subota, S., & Reshetnyak, V. (2008). Surface-induced nonlinearities of liquid crystals driven by an electric field. *Phys. Rev. E*, 78, 061706.
- [10] Hong, Li, Yu, Liang, & Khoo, I. C. (1994). Transient laser induced orthogonal director axis reorientation in dye-doped liquid crystal. *Mol. Cryst. Liq. Cryst.*, 251, 85.
- [11] Khoo, I. C., Min-Yi, Shih, Wood, M. V., Guenther, B. D., Chen, P. H., Simoni, F., Slussarenko, S., Francescangeli, O., & Lucchetti, L. (1999). Dye-doped photorefractive liquid crystals for dynamic and storage holographic grating formation and spatial light modulation. *IEEE Proceedings Special Issue on Photorefractive Optics: Materials, Devices and Applications. IEEE Proceedings*, 87(11), 1897–1911.
- [12] Khoo, I. C., Slussarenko, S., Guenther, B. D., & Wood, W. V. (1998). Optically induced space charge fields, DC voltage, and extraordinarily large nonlinearity in dye-doped nematic liquid crystals. *Opt. Letts*, 23, 253–255.
- [13] Khoo, I. C. (1982). Optical bistability in nematic film using self-focusing of light. *Appl. Phys. Letts.*, 41, 909–911.
- [14] Khoo, I. C. (1983). Re-examination of the theory and experimental results of optically induced molecular reorientation and nonlinear diffractions in nematic liquid crystals: Spatial frequency and temperature dependence. *Phys. Rev.*, A27, 2747–2750.
- [15] Khoo, I. C., Finn, G., Michael, R. R., & Liu, T. H. (1986). Passive optical self-limiter using laser induced axially symmetric and asymmetric transverse self-phase modulations in a liquid crystal film. *Optics Letters*, 11, 227–229.
- [16] Khoo, I. C., Yan, P. Y., & Liu, T. H. (1987). Nonlocal transverse dependence of optically induced director axis reorientation of a nematic liquid crystal film—theory and experiment. *J. Opt. Soc. Am.*, B, 4, 115.
- [17] Khoo, I. C. (1990). Optical amplification and polarization switching in a birefringent nonlinear optical medium: An analysis. *Phys. Rev. Lett.*, 64, 2273.
- [18] Khoo, I. C., & Li, H. (1994). Nonlinear optical propagation and self-limiting effect in liquid crystalline fiber. *Appl. Phys. B*, 59, 573.
- [19] Khoo, I. C. (1996). Optical-dc-field induced space charge fields and photorefractive-like holographic grating formation in nematic liquid crystals. *Mol. Cryst. Liq. Cryst.*, 282, 53–66.
- [20] Hong, Li, Yu, Liang, & Khoo, I. C. (1994). Transient laser induced orthogonal director axis reorientation in dye-doped liquid crystals. *Mol. Cryst. Liq. Cryst.*, 251, 85.
- [21] Malgosia, Kaczmarek, Andrey, Dyadyusha, Sergei, Slussarenko, & Khoo, I. C. (2004). The role of surface charge field in two-beam coupling in liquid crystal cells with photoconducting polymer layers. *J. Appl. Phys.*, 96, 2616–2623.
- [22] Khoo, I. C., & Shepard, S. (1983). Submillisecond grating diffractions in nematic liquid crystal films. *J. Appl. Phys.*, 54, 5491.

- [23] Peccianti, M., Assanto, G., De Luca, A., Umeton, C., Karpierz, M. A., & Khoo, I. C. (2002). Light self-confinement in planar cells with nematic liquid crystals. *J. Communications Technology and Electronics*, 47(7), 790.
- [24] Assanto, G., Peccianti, M., Umeton, C., De Luca, A., & Khoo, I. C. (2002). Coherent and incoherent spatial solitons in bulk nematic liquid crystals. *Mol. Cryst. Liq. Cryst.*, 375, 617–629.
- [25] Khoo, I. C., Jae-Hong, Park, & Justin, Liou (2007). All-optical switching of continuous wave-microseconds lasers with a dye-doped nematic liquid crystal. *Appl. Phys. Letts.*, 90, 151107.
- [26] Khoo, I. C., Park, J. H., & Liou, J. D. (2008). Theory and experimental studies of all-optical transmission switching in a twist-alignment dye-doped nematic liquid crystal. *J. Opt. Soc. Am.*, B25, 1931–1937.
- [27] Khoo, I. C., Wood, M. V., Guenther, B. D., Min-Yi, Shih, Chen, P. H., Zhaogen, Chen, & Xumu, Zhang (1998). Liquid crystal film and nonlinear optical liquid cored fiber array for ps-cw frequency agile laser optical limiting application. *Optics Express*, 2(12), 471–82.
- [28] ANSI Standard Z136.1. American National Standard for the Safe Use of Lasers.